

NUMERICAL SIMULATION AND INDUSTRIAL PRACTICE OF INCLUSION REMOVAL FROM MOLTEN STEEL BY GAS BOTTOM- BLOWING IN CONTINUOUS CASTING TUNDISH

Z. Meijie, G. Huazhi, H. Ao, Z. Hongxi and D. Chengji

Wuhan University of Science and Technology, the Hubei Province Key Laboratory of
Refractories and Ceramics, Wuhan 430081, China

(Received 20 January 2011; accepted 20 April 2011)

Abstract

Gas blowing at the bottom of tundish is an efficient metallurgy technique in clean steelmaking. In this paper, the removal of small size inclusions in the gas bottom-blowing tundish was studied by numerical simulation and industrial practice. The residence time distribution (RTD) of molten steel in the tundish was calculated by mathematical modeling. The content of small size inclusions in the slab was analyzed using a oxygen probing and metallographic images. The results show that the molten steel characteristics obviously change when applied gas bottom-blowing, the average residence time of molten steel in the tundish prolongs more than 100s and the dead volume fraction decreases about 5%. Therefore, the removal efficiency of small size inclusions greatly increases because of bubbles attachment and long moving path. Industrial experiment results show that the average inclusions content of less than 20 μ m decreases more than 24%, the average overall oxygen content decreases about 15% when controlling the reasonable blowing parameters.

Keywords: Tundish; Inclusion removal; Gas blowing; Modeling; Industrial practice.

1. Introduction

The tundish plays an important role in clean steel making by removing some unwanted inclusions from molten steel. So, various kinds of flow control devices (FCD),

such as dam, weir, baffles and turbulence inhibitor (TI) have been developed in recent decades [1-3]. In addition, some new methods have also been proposed in continuous casting process including plasma heating for maintaining appropriate casting

Corresponding author: major6886@gmail.com

steel temperature [4,5], centrifugal flow tundish [6], swirling flow tundish [7] and gas bottom-blowing [8-10]. In these renovations, gas bottom-blowing has attracted more attentions because of higher removal efficiency for small size particle inclusions and low investment. The inert gas was injected through porous brick at the bottom of tundish. Gas bubble curtains are formed. Wei et al [11] have demonstrated through the cold model study that when the particles are not wetted by the liquid, they can be captured by gas bubbles and floated up to the free surface. Solid inclusions such as alumina and silica are not wetted by the liquid steel and therefore can be removed by attachment to gas bubbles. Wang et al [12] have developed a mathematical model to determine the optimum bubble size for the removal of inclusions from molten steel by flotation. The model suggests that the optimum bubble sizes for the removal from steel of alumina inclusions smaller than 50×10^{-6} m in size are in the range of 0.5 to 2×10^{-3} m in diameter. On the basis of studies of particle-gas interaction in water based mineral processing

systems, Lifeng Zhang and S. Taniguchi [13] discussed the mechanism of inclusion removal by bubbles. The overall process of inclusion flotation in steel by a gas bubble can be divided into subprocesses: (1) approach of a bubble to an inclusion; (2) formation of a thin liquid film between inclusion and bubble; (3) oscillation and / or sliding of the inclusion on the bubble surface; (4) drainage and rupture of the film with the formation of a dynamic three-phase contact; (5) stabilisation of the bubble-inclusion aggregate with respect to external stresses; (6) flotation of the bubble-inclusion aggregate. Then a simple mathematical model of inclusion removal by bubble flotation was described.

The contribution of gas bubbling curtains in the tundish to the removal of small size particles has been verified by physical and mathematical modeling [14-16]. In this subject, the flow field, RTD curves and inclusion removal efficiency were analyzed by mathematical modeling at first, then the industrial experience was experimented in Laiwu IRON and Steel Lmtd. The average

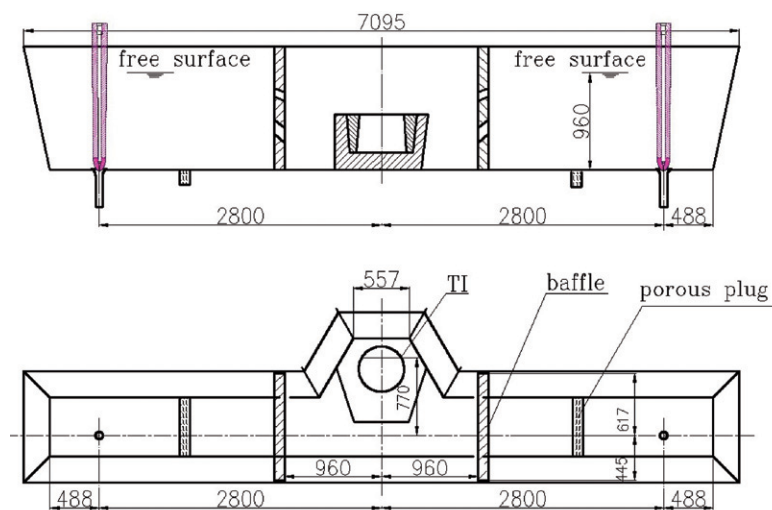


Fig. 1. Geometric dimensions of the industrial tundish

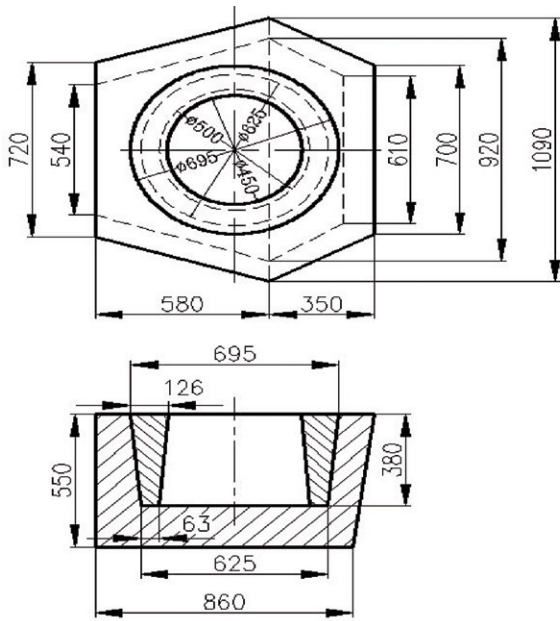


Fig. 2. Geometric dimensions of the TI

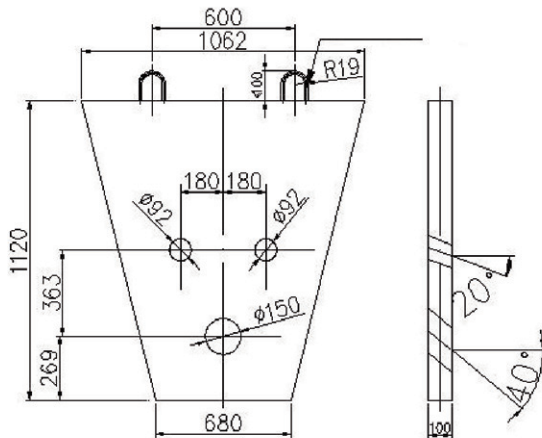


Fig. 3. Geometric dimensions of the baffle

contents of overall oxygen and small size (<math><20\mu\text{m}</math>) inclusions were detected.

2. Description of the industrial tundish

The selected tundish for the present analysis is a 30t tundish of Lai Wu Iron & Steel Ltd., China. The dimensions of this tundish is shown in Figure 1. This two-strand tundish was equipped with a turbulence inhibitor (TI) and a pair of baffles whose dimensions were shown in Figure 2 and Figure 3 respectively. Under steady state conditions, the liquid steel depth in the tundish is 0.96m. The inner diameters of ladle shroud and submerged nozzle are 70mm and 50mm respectively. The numerical simulation was performed for casting slabs (175×1260mm) with casting speed $1.4\text{m}\cdot\text{min}^{-1}$.

In order to study the effect of gas bottom-blowing on removal of inclusions, a pair of porous plugs were established on the bottom of the tundish. Dimensions of the plug were shown in Figure 4.

2.1. Mathematical model

Control equations. A three-dimensional, steady, turbulent bubbly flow in the tundish

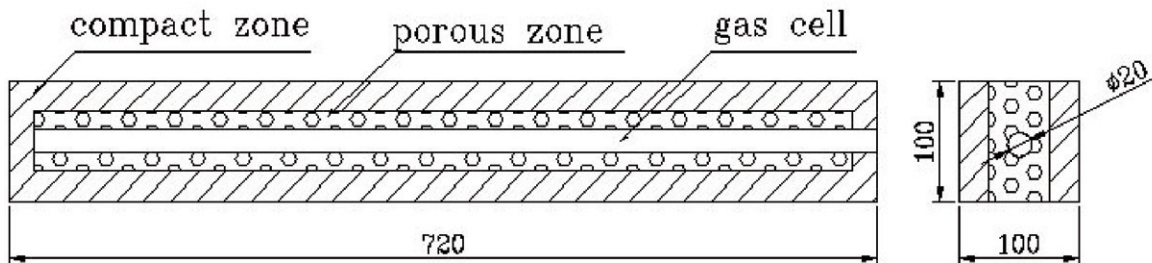


Fig. 4. Schematic of gas curtain bricks for industrial tundish

was simulated using the Eulerian-Eulerian two-phase flow model [10], which molten steel was considered as the primary phase and gas as the secondary phase. The continuity and momentum equations for each phase were solved together with the standard $k-\varepsilon$ turbulent model for liquid steel. The Porous media model was used for gas flow through the porous brick [17]. The viscous resistance factor and inertial resistance factor of gas flow through the brick were acquired by the method for measuring permeability of refractory products [18, 19]. The equation for residence time distribution (RTD) is a normal species transportation equation. Inclusion trajectories were calculated using the discrete phase model (DPM) which solves a transport equation for each inclusion particle as it travels through the previously calculated, steady-state, flow field of molten steel and argon gas.

2.2. Boundary conditions

The boundary conditions for momentum transfer to all solid surfaces, including walls and bottom of tundish, surfaces of baffles and TI were those of non-slipping. Wall functions described by Anderson [20] are used at nodes close to all solid walls. The interface of slag and molten steel is considered as free surface. Velocity gradients, turbulent kinetic energy and its dissipation rate were assumed zero on the free surface and at all solid surfaces. At the liquid inlet, a uniform normal velocity profile was assumed and the average velocity was fixed according to the flow rate. k and ε were specified using the semi-empirical equations [21]. Outflow was set at the liquid

outlet. The density and viscosity of molten steel were assumed constants: 6940kg/m^3 and $0.06239\text{Pa}\cdot\text{s}$.

At the gas inlet, the gas injection superficial velocity was specified from the gas flow rate and the region area of porous refractory, the liquid volume fraction was set as zero. According to the water modeling and past research works [14, 22], the bubbles were assumed as spherical shape and their diameters were assumed as 2mm. The density and viscosity of hot argon gas were assumed constants: 0.342kg/m^3 and $5.741\text{e-}05\text{ Pa}\cdot\text{s}$.

Ideal absorption was assumed at the top surface. At the tundish wall, only a part of inclusions were adopted. Inclusions were assumed to be spherical and the density was 2750 kg/m^3 . The inclusion distribution was the same as reference [23] ranged from 10 to $150\mu\text{m}$. The removal probability of bubbles to inclusions was considered according to reference [14]. The validity of the above mathematical model has been verified by water modeling [14].

All the equations were calculated simultaneously by commercial software CFX. After getting the steady fluid flow, inclusions were injected into the tundish from the inlet. Ten simulations for each case of inclusions trajectories were performed including 1200 particles. The trajectory of each particle was calculated. The total number of injected particles was written as N_t , the number of absorbed particles for different size by the walls was written as $N_{a,i}$, the number of particles for different size floated to the free surface was written as $N_{f,i}$. The different size inclusion removal efficiency can be calculated as:

$$\eta_{t,i} = (N_{f,i} + N_{a,i}) / N_t \quad \dots(1)$$

2.3. Industrial operation and practice

The industrial experiments of gas bottom-blowing in the tundish have been taken in Lai Wu Iron & Steel Ltd. TI and two baffles were established in the tundish as Figure 1. The porous brick was established at the bottom of tundish. In order to compare the results of gas blowing, only at one side of the tundish bottom, porous brick was established which was shown in Figure 5. The argon gas was injected into the tundish just before the opening of the first ladle of the sequence. The argon gas flow rate was controlled below 4.0 Nm³/h, which makes a stable slage layer. Samples carried out from slabs with gas bubbling side were marked as A group and B group represented samples without gas bubbling. For each side slab, a group samples were carried out at three different positions: central—sample 1, quarter—samples 2, exterior—sample 3. The detailed samples positions were shown in Figure 6. Each group of samples was carried out every 4mins for each side slab. 30 samples of A and 30 samples of B were collected.

All the samples were evaluated by optical

microscopy. Metallographic preparation was performed according to ASTM standards. The inclusion size distribution was measured in terms of number of inclusions per mm² of steel sample area. A total of 50mm² area was observed in each sample. 30 samples were averaged for samples A and samples B. Oxygen content for all the samples were detected by Oxygen Sensor. The average oxygen contents of samples A and samples B were calculated. The average mass fraction of oxygen for samples A was recorded as O_A , while that for samples B was recorded as O_B . The decreasing efficiency of oxygen content in the steel slab with gas bottom bubbling was calculated as:

$$\eta = \frac{O_A - O_B}{O_A} \times 100\% \quad \dots(2)$$

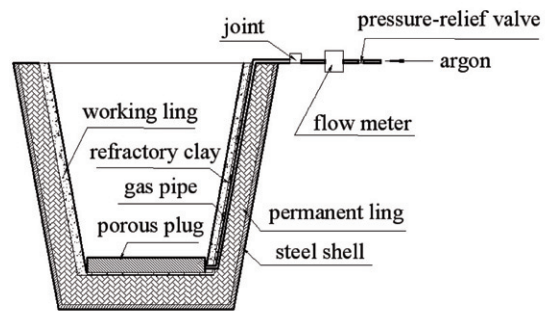


Fig. 5. Schematic installation diagram of porous refractory in the tundish

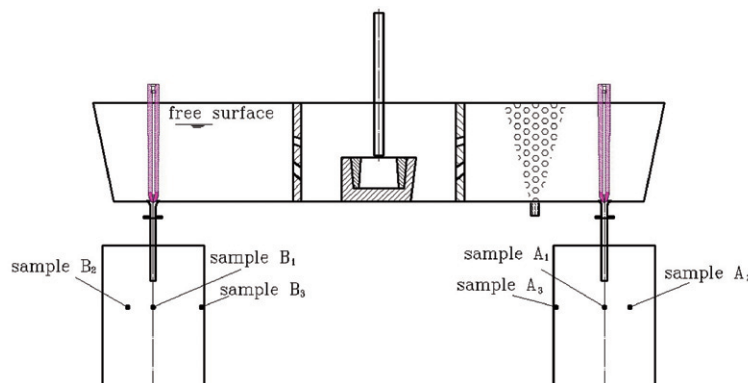


Fig. 6. Samples positions

3. Results and discussion

Fluid flow. The pathlines of molten steel flow in the tundish are shown in Figure 7. Figure 7 (a) corresponds to the tundish without gas blowing. Figure 7 (b) corresponds to the tundish with gas bottom-blowing, which the gas flow rate is $3.6\text{Nm}^3/\text{s}$, the gas blowing position is 2260mm from inlet axis.

Figure 7 shows a heavy fluid mixing with high turbulence in the inject zone and has no obvious difference for both cases. The mixing turbulent flow increases the collision

of inclusions. Through the holes on the baffle, the molten steel are divided into three parts without gas blowing: one part flow to the top surface and then flow out along the stopper; one part make a backflow between the stopper and the baffle; another part can not reach the top surface and directly flow to the outlet. When gas was blowing from the bottom of tundish, the molten steel flow patten changes obviously: two backflows at each side of gas bubbles curtain are formed, the flowing paths greatly prolong. This flow characteristics will increase the residence time of molten steel in the tundish.

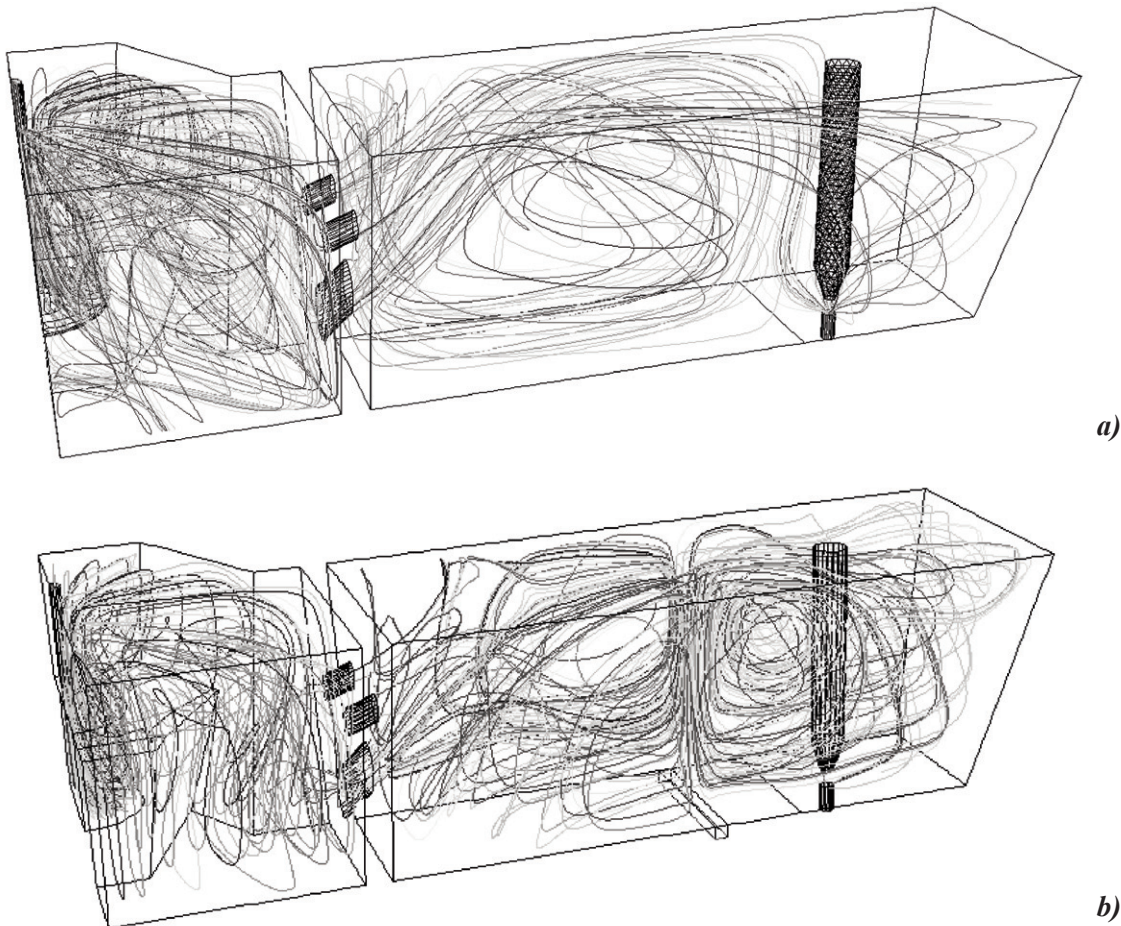


Fig. 7. Pathlines of molten steel flow in the tundish (a- without gas bubbling, b- with gas bubbling)

RTD curves and analysis. RTD curves have been widely used to analyze the flow characteristics in the continuous tundish [24]. Figure 8 shows the RTD curves for the tundish with different FCD. Analysis of RTD curves is shown in Table 1. In Figure 8, C presents dimensionless concentration of tracer in the tundish while θ presents dimensionless time.

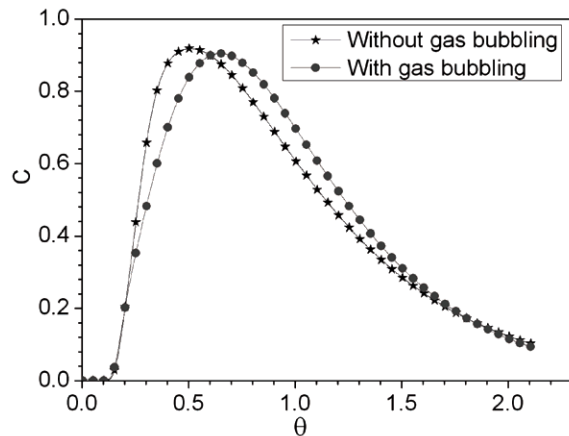


Fig. 8. RTD curves of molten steel in the tundish with different FCD

It is known from Figure 8 and Table 1 that the curves are fairly similar in shape and the minimum residence times (t_{\min}). But the peak concentration time (t_{peak}) and the average residence time (t_{av}) are much higher

Table 1. Analysis of RTD curves shown in figure 8

	t_{\min} , s	t_{peak} , s	t_{av} , s	V_d/V , %	V_p/V , %	V_m/V , %
Without gas bubbling	118	505	878	19.7	31.2	49.1
With gas bubbling	114	646	981	15	38.1	46.9

with gas bottom-blowing compared with no gas bubbling. So, the dead volume fraction (V_d/V) decreases from 19.7% to 15.0% with gas bubbling. The differences of RTD curves indicate gas bottom-blowing would significantly increase inclusion removal efficiency because of long residence time.

Inclusion removal analysis. Figure 9 shows the trajectories of overall inclusions (10~150 μm) in the gas bubbling tundish and without gas bubbling tundish. Figure 10 shows the inclusion removal efficiency of different size particles in the different tundishes.

It can be seen that the inclusions trajectories almost identical in the inject zone for both tundishes. After flowing through the holes on the baffle, some particles flow to the free surface with molten steel, the large size particles float up to the surface at the Stoke's force, the small size particles cannot reach the top surface and flow out with the liquid without gas bubbling shown as Figure 9 (a). When gas is blowing from the bottom of tundish, some small size particles are attached to the bubbles and float up to the surface shown as Figure 9 (b). So, the removal efficiency of small size inclusions (~20 μm) increases greatly (from 0 to more than 30%) shown as in Figure 10. For the large size particles (50 μm ~), there is no significant influence on the removal efficiency with gas bottom-blowing. In the case of small size particles (~20 μm), the removal efficiencies obviously enhanced. So, the main contribution of gas bubbling is removing the micro-inclusions.

The previous studies have verified that the gas flow rate and gas blowing position have

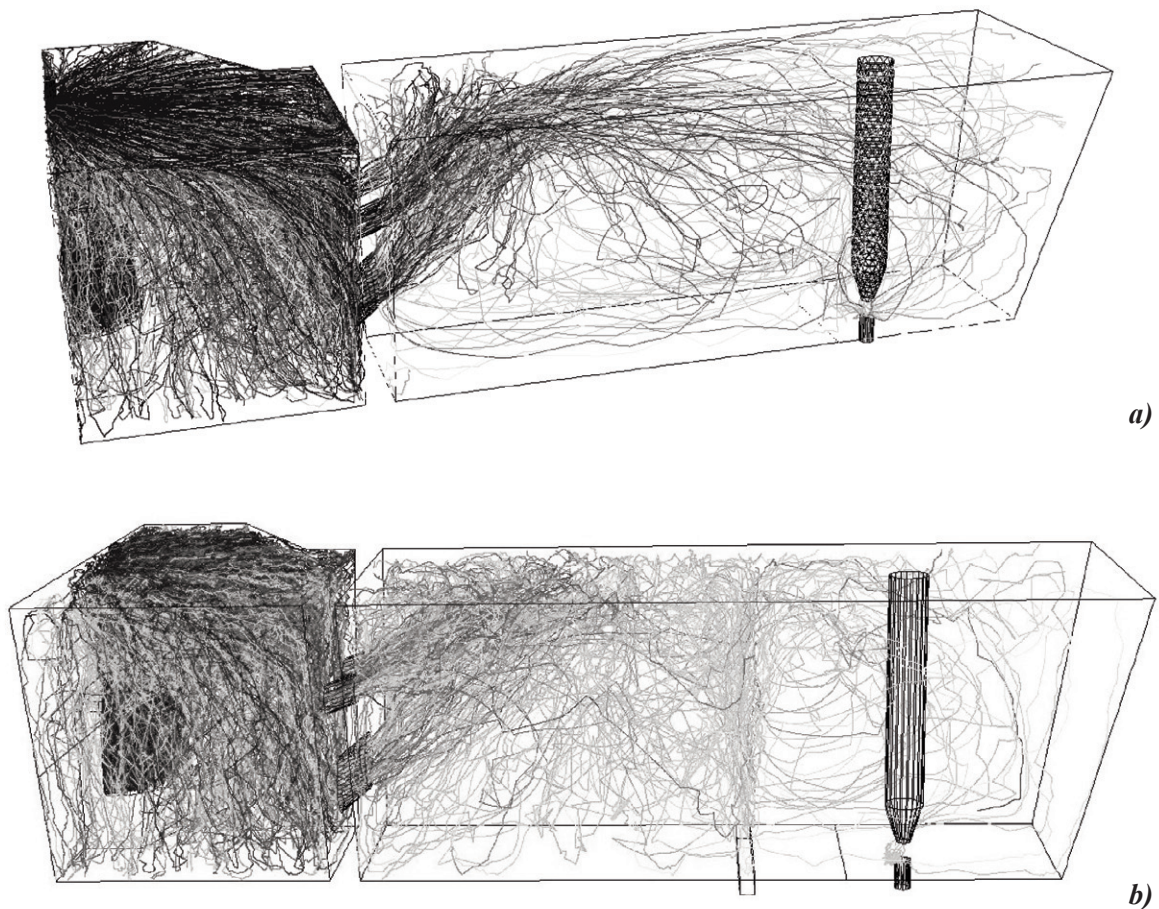


Fig. 9. Pathlines of inclusion particles
(a- with gas bubbling, b- without gas bubbling)

great effect on the flow characteristics and inclusion removal efficiency [9, 25]. In the current work, flow field and inclusion removal efficiencies were modeled for different gas bottom-blowing position and at different gas flow rate from 2.1 to 5.25 Nm^3/s . The influence of gas flow rate and bubbling position on inclusion removal efficiencies are shown in Figure 11 and Figure 12 respectively. The gas bubbling position is 2.26m from inlet correspond to Figure 11. For Figure 12, the gas flow rate was fixed to 4.2 Nm^3/s . The corresponding flow fields are not given here.

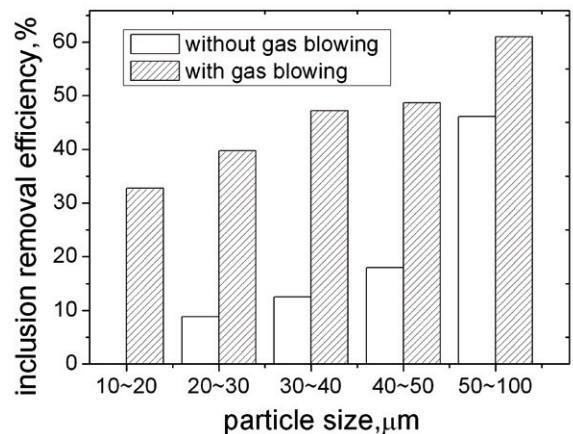


Fig.10. Comparison of removal efficiency of different size particle

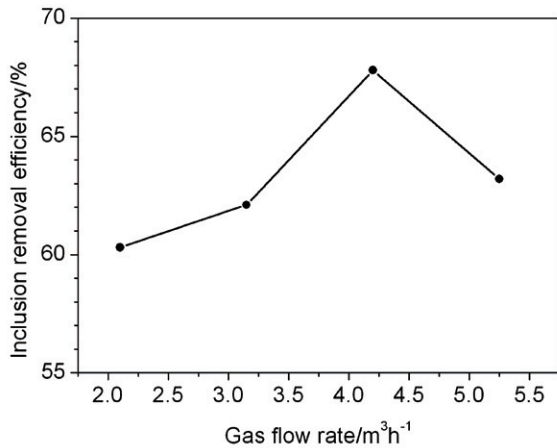


Fig. 11. Inclusion removal efficiencies at different gas flow rate

It can be concluded from Figure 11 that the inclusion removal efficiency increases with gas flow rate increase below the 4.2 Nm³/s. When the gas flow rate is higher than 4.2 Nm³/s, the inclusion removal efficiency decreases because the velocities near up surface are so high that the inclusions are entrapped into the liquid. We can concluded from Figure 12 that the gas position should not be too near to the outlet, the optimum gas bubbling position is 2.26m from the inlet.

Industrial analysis. Based on the numerical simulations of the tundish, the industrial experiments of gas bottom bubbling in the tundish have been taken in Lai Wu Iron & Steel Ltd. The variations of oxygen content are shown in Figure 13. The SEM pictures of samples are shown in Figure 14.

For samples made from slab without gas blowing, there are inclusions in the case of 100 μm seen from Figure 14(b). For samples made from slab with gas blowing, inclusion which size is more than 60μm has not been seen. In this subject, only less than 20 μm

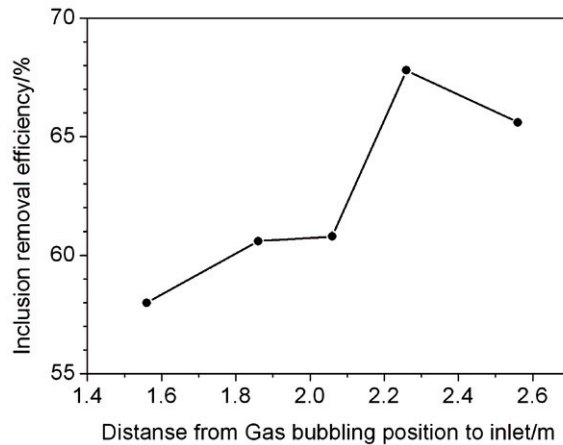


Fig. 12. Inclusion removal efficiencies at different gas bubbling position

inclusions were statistically analyzed. The average inclusions content of less than 20μm decreases more than 24% for gas blowing slab shown as in Figure 13. And the average overall oxygen content decreases about 15%. The results predicted by mathematical modeling were more than obtained from engineering practice. The deviations are mainly caused by some assumptions such as (1) the inclusions are totally absorbed by the surface slag, (2) the bubbles coalescence is

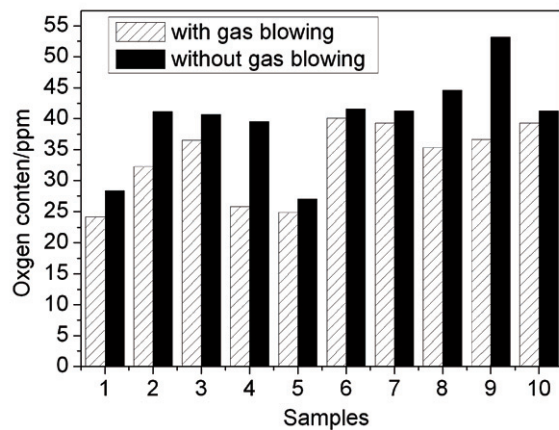


Fig. 13. Oxygen content of samples

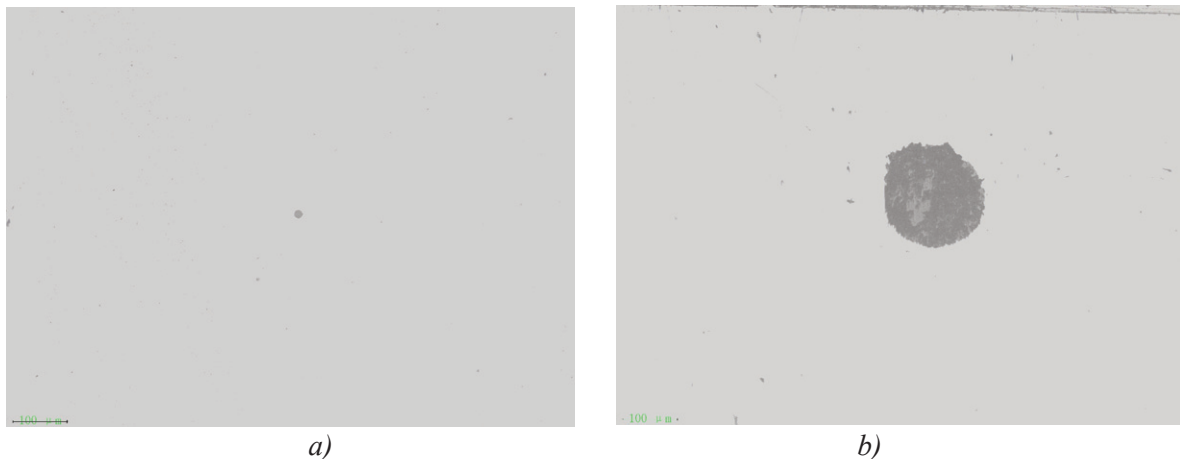


Fig. 14. SEM pictures of samples (a-with gas blowing, b- without gas blowing)

neglected. The industrial practices verify that applying gas curtain technique can increase the small size inclusions removal.

4. Conclusions

The efficiency for promotion removals of inclusions in the gas bottom-blowing tundish were studied using numerical simulation, and valications were carried in industrial experiments. The main conclusions derived from this study are as follows.

(1) Using Eulerian-Eulerian and DPM model, the liquid-gas flow, RTD curves, inclusion trajectories and the removal efficiency were numerically calculated. The results show the average residence time of molten steel in the tundish prongs, the dead volume fraction decreases with gas bottom-blowing in the tundish.

(2) With gas bottom-blowing in the tundish, some small size particles adhered to the bubbles and floated up to the surface when encountering the gas bubbles curtain. So the removal efficiency of large size particles has no obvious changes, the gas

bottom-blowing has great contribution to the removal of small size particles.

(3) Flow field and inclusion removal efficiencies were modeled for different gas bottom-blowing positions and at different gas flow rates from 2.1 to 5.25 Nm³/s. Based on the results, the optimum gas flow rate and gas bubbling position were determined.

(4)The gas bottom-blowing in the tundish was taken into industrial practice . The content of small particle size inclusions in the slab was analyzed using a oxygen probing and metallographic images. The results show that the average inclusions content of less than 20μm decreases more than 24%, the average overall oxygen content decreases about 15% when controlling the reasonable blowing parameters.

Acknowledgments

This work is supported by the State Key Development Program for Basic Research of China (2009CB62600) and Natural Science Foundation of Hubei Province of China(2009CDZ010) and (2009CDB042).

References

- [1] Liangcai Zong, Baokuan Li, Yingxiong Zhu, Rengui Wang, Wenzhong Wang and Xiaojun Zhang, ISIJ Intern. 47 (1) (2007) 88
- [2] Pardeep K. JHA, P. Srinivasa RAO and Anupam DEWAN, ISIJ Intern. 48 (2) (2008) 154.
- [3] P. Gardin, M. Brunet, J.F. Domgin and K. Pericleous, Appl. Math. Modeling. 26 (2002) 323.
- [4] Setsuo KITAKA, Shuji WAKIDA, and Toyohiko KANKI, Nippon steel technical report. 85 (2002) 162.
- [5] J. de J. Barreto-sandoval, A. W. D. Hils, M. A. Barreto-meza, ISIJ Intern. 36 (1996) (9) 1174.
- [6] Yun Wang, Yunbo Zhong, Baojun Wang, ISIJ Intern. 49 (10) (2009) 1542.
- [7] Qinfu Hou, Qiang Yue and Huanyang Wang, ISIJ Intern. 48 (6) (2008) 787.
- [8] J.P. Rogler, L.J.Heaslip and M.Mehrvar, Canadian Metallurgical Quarterly. 44 (2005) 357.
- [9] A. Ramos-Banderas and R.D.Morales, ISIJ Intern. 43 (5) (2003) 653.
- [10] Zhang Meijie, Wang Houzhi, Gu Huazhi and Huang Ao, Journ. Iron and Steel Res. 19 (2) (2007) 16. (*in Chinese*).
- [11] P. Wei, K-I. Uemura and S.K. Oyama, Tetsu-to-Hagane. 78 (1992) 1361 (*in Japanese*).
- [12] Wang Laihua, Hae-Geon LEE and Peter Hayes, ISIJ Intern. 36 (1) (1996) 17.
- [13] Lifeng Zhang and S.Taniguchi, Intern. Mater. Rev. 45 (2000) 59.
- [14] M. J. Zhang, H. Z. Gu, A. Huang, H. X. Zhu and C. J. Deng, Min. Metall. Sect. B-Metall. 47 B (2011) (1) 37.
- [15] A. Ramos-Banderas, R.D. Morales and J. de J. Barreto, Steel Research. 77 (5) (2006) 325.
- [16] Wang Litao, Zhang Qiaoying and Li Zhengbang, Journ. Iron and Steel Res, Intern. 11 (6) (2004) 5 (*in Chinese*).
- [17] Meijie Zhang, Huazhi Gu, Ao Huang, Journ. Iron and Steel Res, Intern. 20 (2008) 13 (*in Chinese*).
- [18] Meijie Zhang, Houzhi Wang, Huazhi Gu and Ao Huang, Key Eng. Mater. 368-372 (2008) 1155.
- [19] Meijie Zhang, Houzhi Wang, Huazhi Gu and Ao Huang, Journ. Wuhan University of Sci. & Tech. (Natural Science Edition). 2008, 31 (3) 284 (*in Chinese*)
- [20] Anderson D. A., Tannehill J. C., Pletcher R. H., Computational fluid mechanics and heat transfer, Mc Graw-Hill Books Co., New York N.Y., (1984) p. 357
- [21] D. Mazumdar, R.I.L. Guthrie, ISIJ Intern. 39 (6) (1999) 524.
- [22] Hua Bai. Ph. D thesis. USA: University of Illinois at Urbana-Champaign, 2000.
- [23] Asish Kumar Sinha, Yogeshwar Sahai, ISIJ Intern. 33 (5) (1993) 556.
- [24] Dipak Mazumdar and Roderick I.L.Gutrie, ISIJ Intern. 39 (5) (1999) 524.
- [25] R. H.Yoon and G.H.Luttrell. Min, Processing and Extractive Metall. Rev. 5 (1989) 101.